Regional 2-[^{18}F]fluoro-2-deoxy-D-glucose uptake varies in normal lung

Tsutomu Miyauchi, Richard L. Wahl

Division of Nuclear Medicine, Department of Internal Medicine, University of Michigan, Ann Arbor, Michigan, USA

Received 2 October and in revised form 23 December 1995

Abstract. 2-[^{18}F]fluoro-2-deoxy-D-glucose positron emission tomography (FDG-PET) is a promising imaging procedure for detecting primary and metastatic cancer in the lungs. We have, however, failed to detect some small tumors in the lower lobes of the lungs. This study aimed to determine whether increase ^{18}F background activity in the dependent lower lungs is present, which could make lesion detection more difficult. We measured the standardized uptake values (SUVs) for FDG of normal lung remote from the nodular lesion in 16 patients with newly diagnosed untreated lung lesions stronlgy suspected to represent non-small cell lung cancers. In addition, 15 patients with known or suspected primary breast cancers without pulmonary lesions were included as control subjects. After PET transmission images of the thorax were obtained, approximately 370 MBq of FDG was injected intravenously and imaging was immediately begun. Patients were supine throughout the study. SUVs were determined with images obtained 50–70 min after FDG injection. Regions of interest (ROIs) of 6×6 pixels were positioned over normal lung in anterior, mid, and posterior portions of upper, middle, and lower lung fields. Thus, as many as 18 ROIs were positioned in each patient. The SUVs of the posterior portion were significantly higher than those of the anterior and mid portions in the population of 31 cases (P <0.001). Also, the mean SUV of the lower lung field was significantly higher than the SUVs of the upper and middle lung fields in this population (P <0.01). This pattern was seen among the two groups of 16 patients suspected of having lung cancer and 15 control subjects. Background ^{18}F activity was highest in posterior and lower lung in these patients. The maximum value of mean SUV observed in normal posterior lower lung was 0.804±0.230 (41% greater than the mean SUV in the anterior upper lung), which is in the range of the apparent SUV for a 5-mm lung lesion, with higher SUV, due to recovery coefficient issues. Thus this phenomenon could contribute to occasional false-negative lesions in those areas. Increased blood flow and FDG delivery and also scatter from heart and liver may contribute to the increased lower lung background activity. Regional differences in normal lung FDG uptake are significant and should be considered when interpreting pulmonary PET studies in patients with suspected primary or metastatic lung cancer.

Key words: Positron emission tomography – Lung – 2-[^{18}F]fluoro-2-deoxy-D-glucose – Standardized uptake value

Eur J Nucl Med (1996) 23:517–523

Correspondence to: R.L. Wahl, Division of Nuclear Medicine, University of Michigan Medical Center, 1500 E Medical Center Dr., B1G 412, Ann Arbor, MI 48109-0028, USA

Introduction

Lung cancer is a leading and growing cause of morbidity and death in men and women throughout the world. To achieve cure, it is important to detect lung cancer in its early stages. Most diagnostic procedures such as computed tomography (CT) and magnetic resonance imaging depend on anatomical change, so it is not easy to differentiate benign from malignant pulmonary lesions especially when they are small and/or solitary. In addition, the lungs represent a major site for metastases from many types of cancer.

Glucose metabolism of cancer cells is generally increased [1–3]. 2-[^{18}F]fluoro-2-deoxy-D-glucose (FDG) is a positron-emitting glucose analogue, and following intravenous injection, FDG accumulates rapidly in many malignant tumors [4]. Positron emission tomography (PET) using FDG yields metabolic information which can assist in tissue characterization. FDG-PET is a promising imaging technique in differentiating malignant from benign pulmonary nodules and in detecting/characterizing metastatic tumors to lung and lymph nodes. However, we recently failed to detect several small malignant metastatic lesions in the lower lung field in patients with melanoma, a tumor which generally has very high levels of glucose metabolism [5]. To determine whether this occasional difficulty in detecting small lung lesions is due to increased background ^{18}F activity in the lower lungs, we measured regional uptake of

FDG in varying regions of clinically normal lungs retrospectively.

Materials and methods

Patients and subjects. Sixteen patients (11 men and five women) with newly diagnosed untreated lung lesions strongly suspected to represent non-small cell lung cancers were included in this study. Patients ranged in age from 42 to 76 years (mean±SD, 61.3±10.1). None had a history of diabetes or heart failure or had obvious ongoing pulmonary infection, though most had a history of cigarette smoking. The control subjects consisted of 15 women with known or suspected primary breast cancers without pulmonary nodules or cardiovascular disease (age range 37–68 years; mean±SD, 53.3± 9.8).

FDG production. ^{18}F was produced with a T.C.C. model CS-30 cyclotron (Cyclotron Corporation of America, Berkeley, Calif.) by the acceleration of protons into an $H_2{}^{18}O$ target. FDG of high specific activity (>3000 Ci/mmol) was produced by means of nucleophilic fluorination [6]. Purity was assessed by means of thin-layer chromatography and high-performance liquid chromatography. Methods of production were in accordance with those for an investigational new drug registered with the U.S. Food and Drug Administration.

PET scanning. PET images were acquired with an ECAT 921/EXACT scanner (CTI, Knoxville, Tenn., distributed by Siemens Medical Systems, Iselin, N.J.) for 14 patients and 15 control subjects. For two patients PET was performed with an ECAT 931/08 scanner (CTI). The scanning protocol was similar to one we have previously described for imaging of breast, genitourinary tract cancers, and lymphomas [7–9]. We obtained 47 transverse planes of 3.4-mm thickness encompassing a 16.0-cm axial field of view with the ECAT 921 scanner. Fifteen transverse planes with a 6.75-mm thickness and a 10.3-cm axial field of view were obtained with the ECAT 931 scanner.

Patients were fasted for at least 4 h before imaging. Transmission scanning with a germanium-68 ring or rod source was performed at two levels of the thorax. These images generally included the whole thorax for the ECAT 921 scanner. After the transmission images were obtained, we injected approximately 370 MBq of FDG intravenously and began emission imaging. We obtained 17 dynamic images from the time of injection until 60 min after injection at the primary imaging level. These images included six 10-s frames, three 20-s frames, two 90-s frames, one 5-min frame, and five 10-min frames. For the second attenuation-corrected imaging level, we obtained static images at 60–70 min after injection. Patients were supine throughout the study. Since this was a retrospective study, data from the prone position were not obtained.

Quantitative image analysis. Images were reconstructed with a 128×128 matrix by using a filtered back-projection algorithm with a Hanning filter cut-off value of 0.3. The voxel size of the ECAT 921 scanner was 4.2×4.2×3.4 mm, while for the ECAT 931 scanner it was 4.7×4.7×6.75 mm. The reconstructed x-y resolution was approximately 10 mm full-width at half-maximum in plane for both scanners. The reconstructed z-axis resolution was about 5 mm for the ECAT 921 scanner and 7.5 mm for the ECAT 931 scanner. The FDG standardized uptake values (SUVs) were determined for images obtained 50–70 min after FDG injection. SUV, rather than the preferred SUV lean, was obtained as statistical comparisons were by paired test in the same patients and because patients were generally not obese [10]. Quantitation of FDG uptake by normal lung was performed with a computerized analysis system (IVAS). First of all, a 6×6-pixel region of interest (ROI) was positioned over normal lung in anterior, mid and posterior portions of the upper (aortic arch level), middle (carinal level) and lower lung fields in the transmission images. Then, these ROIs were copied to the spatially registered emission images at the same level. Thus, as many as 18 ROIs were positioned in each patient (Fig. 1). We did not include any pulmonary lesions, myocardium or chest wall within these ROIs. SUVs were calculated from two 10-min acquisitions (50–60 min post injection and 60–70 min post injection). The relation between the levels at which SUVs were measured and time after injection is shown in Table 3 for each patient as a part of the imaging summary. Analysis of variance (ANOVA) with repeated measures (post hoc test was performed by Scheffe's F test) was employed for the comparison of SUVs in anteroposterior and craniocaudal locations. For the comparison of the SUVs between the right and left lobes, the paired t-test was performed. Statistical results were considered to be significant when $P < 0.05$. P values of the paired t-test are two-tailed.

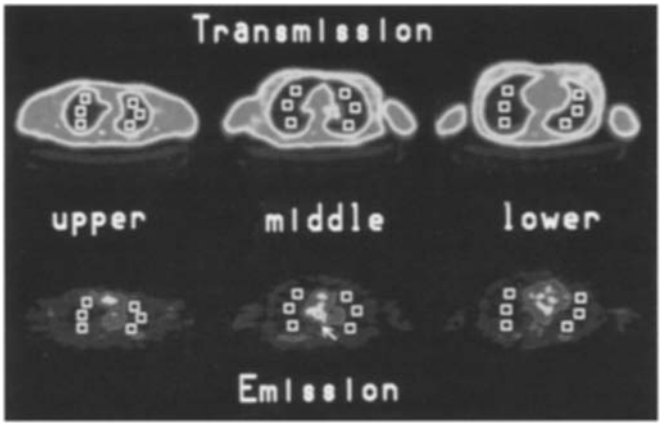

Fig. 1. Multiple 6×6 pixel ROIs are positioned in the anterior, mid, and posterior portions of the upper, middle, and lower lung fields. ROIs were positioned first in transmission images then copied onto spatially registered emission images at the same level. The *arrow* indicates the intense uptake of FDG in the area of a squamous cell carcinoma (patient 11)

Results

Clinical and histologic findings of the patients and control subjects are shown in Tables 1 and 2. All of the patients were smokers (patient 2 was a passive smoker). Mild emphysematous changes were seen on CT scan in 6 of the 16 patients suspected of having lung cancer. According to the pulmonary function tests, four patients had mild airway obstruction (patients 6, 8, 13, and 16). No patient suffered from heart failure at the time of the PET study. Of the control subjects, only two were smokers and none had clinically evident respiratory or cardiac abnormalities at the time of PET. Imaging information is summarized in Table 3.

Table 1. Clinical and histologic findings in 16 patients suspected of having primary lung cancer

Patient no.	Age/sex	Pulmonary nodule	Histologic finding	Smoking history	Baseline CPD	FVC (%)[a]	FEV_1 (%)[a]	Heart failure?
1	44/M	Left lower lobe	Inflammatory pseudotumor	+	Emphysema[b]	100	100	No
2	69/F	Right upper lobe	Granuloma	–[c]	None	85	88	No
3	42/M	Bilateral lower lobe	Granuloma	+	Emphysema[b]	104	103	No
4	58/M	Left upper lobe	Large cell carcinoma	+	Emphysema[b]	100	69	No
5	65/M	Right lower lobe	Squamous cell carcinoma	+	None	82	86	No
6	56/M	Right middle lobe	Adenocarcinoma	+	Emphysema[b]	75	59	No
7	76/F	Right upper lobe	Adenocarcinoma	+	None	101	97	No
8	58/F	Right upper lobe	Non-small cell type carcinoma	+	None	72	61	No
9	71/F	Right lower lobe	Squamous cell carcinoma	+	None	90	87	No
10	61/M	Left hilum	Small cell carcinoma	+	Emphysema[b]	88	61	No
11	57/F	Right middle/ lower lobe	Squamous cell carcinoma	+	None	108	82	No
12	70/M	Left lingula	Small cell carcinoma	+	None	91	78	No
13	63/M	Right upper lobe	Squamous cell carcinoma	+	None	78	65	No
14	50/M	Right upper lobe	Squamous cell carcinoma	+	None	–	–	No
15	65/M	Right upper lobe	Non-small cell type carcinoma	+	Emphysema[b]	84	62	No
16	75/M	Left upper lobe	Adenocarcinoma	+	None	72	64	No

CPD, Chronic pulmonary disease; FVC, forced vital capacity; FEV_1, forced expiratory volume in 1 s

[a] Values of FVC and FEV_1 are expressed as a percentage of the predicted value

[b] Mild emphysematous changes observed by CT scan

[c] Passive smoker

Table 2. Clinical and histologic findings in 15 control subjects suspected or known to have primary breast cancer without pulmonary lesion

Subject no.	Age/sex	Histologic finding	Smoking history	Baseline CPD	FVC (%)[a]	FEV_1 (%)[a]	Heart failure?
1 C	63/F	Adenocarcinoma	–	None	–	–	No
2 C	46/F	Ductal carcinoma	–	None	–	–	No
3 C	59/F	Ductal carcinoma	–	None	–	–	No
4 C	37/F	Sarcoma	–	None	–	–	No
5 C	59/F	Lobular carcinoma	–	None	–	–	No
6 C	44/F	Ductal carcinoma	+	None	–	–	No
7 C	57/f	Adenocarcinoma	–	None	–	–	No
8 C	46/F	Negative for cancer	–	None	–	–	No
9 C	43/F	Fibroadenoma	–	None	–	–	No
10 C	66/F	Fibrocystic change	–	None	–	–	No
11 C	64/F	Negative for cancer	–	None	–	–	No
12 C	55/F	Lymphofollicular hyperplasia	+	None	–	–	No
13 C	68/F	Negative for cancer	–	None	–	–	No
14 C	44/F	[b]	–	Asthma	92%	95%	No
15 C	49/F	Cyst	–	None	–	–	No

C, Control; CPD, chronic pulmonary disease; FVC, forced vital capacity; FEV_1, forced expiratory volume in 1 s

[a] Values of FVC and FEV_1 are expressed as a percentage of the predicted value

[b] Pathological diagnosis was not obtained for this subject

Table 3. Summary of imaging information for 31 subjects[a]

Patient no.	Scanner	SUV 50–60[b]	SUV 60–70[b]	Subject no.	Scanner	SUV 50–60[b]	SUV 60–70[b]
1	921	Lo	Up, M	1 C	921	M, Lo	Up
2	921	Up, M, Lo	–	2 C	921	M, Lo	Up
3	921	Up, M, Lo	–	3 C	921	M, Lo	Up
4	921	Up, M, Lo	–	4 C	921	M, Lo	Up
5	921	Up, M, Lo	–	5 C	921	M, Lo	Up
6	921	Up, M	Lo	6 C	921	M, Lo	Up
7	921	Up, M	Lo	7 C	921	Lo	Up, M
8	931	Up	–	8 C	921	M, Lo	Up
9	921	Up, M, Lo	–	9 C	921	M, Lo	Up
10	931	M, Lo	–	10 C	921	Up, M, Lo	–
11	921	Up, M, Lo	–	11 C	921	M, Lo	Up
12	921	Up, M, Lo	–	12 C	921	M, Lo	Up
13	921	Up, M	–	13 C	921	Lo	Up, M
14	921	Up, M	Lo	14 C	921	M, Lo	Up
15	921	Up, M	Lo	15 C	921	M, Lo	Up
16	921	Up, M	Lo				

SUV 50–60, SUV data obtained from 50 to 60 min post injection; SUV 60–70, SUV data obtained from 60 to 70 min post injection; Up, upper lung field; M, middle lung field; Lo, lower lung field; C, control

[a] The entire lung field was not imaged for patients 8, 10, and 13

[b] The levels at which SUVs were measured are indicated

Table 4. SUVs in various regions of normal lung as measured in all 31 subjects

	Anterior portion	Mid portion	Posterior portion	Overall
Upper lung	0.569±0.199	0.515±0.218	0.663±0.176	0.583±0.207
Middle lung	0.537±0.166	0.541±0.181	0.675±0.252	0.584±0.212
Lower lung	0.639±0.274	0.679±0.217	0.804±0.230	0.712±0.249
Right lobe	0.595±0.247	0.573±0.224	0.708±0.235	0.625±0.241
Left lobe	0.558±0.175	0.576±0.209	0.719±0.224	0.619±0.214
Bilateral lobe	0.578±0.216	0.575±0.216	0.713±0.229	0.622±0.228

Values are expressed as mean±SD

Regional SUVs in normal lung for the entire population are shown in Table 4. For the entire population, mean SUVs were significantly different in anteroposterior locations, with $P < 0.01$ by ANOVA with repeated measures [mean SUVs of the posterior portion were significantly higher than those of the anterior and mid portions, ($P < 0.01$ by the post hoc test)]. Also, mean SUVs were significantly different in craniocaudal locations, with $P < 0.01$ by ANOVA with repeated measures [mean SUVs of the lower lung field were significantly higher than those of the upper and middle lung fields ($P < 0.01$ by the post hoc text)]. In the paired comparison of mean SUVs between the right and the left lobe, no significant differences were observed except for the mid portion of the middle lung field, where the left lobe showed slightly higher FDG uptake than the right.

Regional SUVs in normal lung for the 16 patients suspected of having lung cancer are shown in Table 5. In these 16 patients, mean SUVs were significantly different in anteroposterior and craniocaudal locations ($P < 0.01$). Paired comparison of mean SUVs between the right and left lobes showed no significant difference.

Regional SUVs in normal lung for the 15 control subjects are shown in Table 6. Mean SUVs were significantly different in anteroposterior and craniocaudal locations, with $P < 0.0001$ by ANOVA with repeated measures. Significant differences were observed between upper and lower lung fields, middle and lower lung fields, anterior and posterior portions, and mid and posterior portions ($P < 0.0001$, $P < 0.05$, $P < 0.001$, and $P < 0.0001$ respectively). Paired comparison of mean SUVs between the right and left lobes showed no significant difference.

In summary, SUVs of normal lung showed a ventrodorsal and craniocaudal gradient in patients imaged with this protocol, with the mean SUV in the lower posterior lung being 41% greater than that in the upper anterior lung field. The highest SUV in normal lung was 1.418 for the 16 patients and 1.576 for the control subjects.

Table 5. SUVs in various regions of normal lung in the 16 patients suspected of having primary lung cancer

	Anterior portion	Mid portion	Posterior portion	Overall
Upper lung	0.624±0.225	0.529±0.258	0.711±0.189	0.623±0.234
Middle lung	0.510±0.177	0.557±0.215	0.626±0.253	0.563±0.219
Lower lung	0.627±0.315	0.691±0.252	0.721±0.227	0.684±0.262
Right lobe	0.597±0.281	0.591±0.283	0.682±0.255	0.625±0.274
Left lobe	0.561±0.176	0.581±0.211	0.688±0.194	0.612±0.201
Bilateral lobe	0.581±0.239	0.586±0.248	0.685±0.226	0.619±0.241

Values are expressed as mean±SD

Table 6. SUVs in various regions of normal lung in the 15 subjects suspected or known to have primary breast cancer

	Anterior portion	Mid portion	Posterior portion	Overall
Upper lung	0.518±0.159	0.503±0.179	0.618±0.153	0.546±0.170
Middle lung	0.564±0.151	0.526±0.145	0.722±0.245	0.604±0.203
Lower lung	0.647±0.247	0.670±0.190	0.882±0.206	0.734±0.238
Right lobe	0.593±0.212	0.559±0.160	0.732±0.215	0.628±0.210
Left lobe	0.556±0.175	0.572±0.210	0.747±0.247	0.625±0.229
Bilateral lobe	0.575±0.195	0.565±0.188	0.739±0.230	0.626±0.219

Values are expressed as mean±SD

Discussion

FDG-PET is promising imaging procedure for detecting and characterizing various kinds of tumors including primary and metastatic cancers of the lungs [11–16]. However, we have occasionally failed to detect some small lung lesions in the lower lobes by FDG-PET with the ECAT 931 scanner [5]. These lesions were close to the diaphragm and liver. While scatter activity, lung motion, and the inferior z-axis resolution of this device, by comparison with the 921 scanner, could cause these findings, we were concerned that the findings might be due, in part, to increased uptake of FDG at the lung bases, making lesion detection more challenging.

Many investigators have previously examined regional variations in normal lung density using CT. During normal tidal ventilation, there exists a significant difference in normal lung density between dependent and nondependent regions of the lung [17, 18]. In the supine position, pulmonary density (Hounsfield units) has been found to slow an anteroposterior gradient (posterior is higher) by CT scan [19, 20].

Using positron emission and transmission tomography, regional values of vascular and extravascular lung density have been measured. Schuster et al. measured regional lung density and lung water in normal and edematous lung in vivo in supine dogs. In their study, there was an anteroposterior gradient (posterior was higher) in lung density, but the ratio of lung water to lung density was constant throughout the lung [21]. In a human PET study using inhaled carbon-11 carbon monoxide, a pronounced anteroposterior gradient (posterior was higher) of both lung and blood density was reported, while the gradient of extravascular lung density was quite small [22]. It is known that FDG uptake can occur into inflammatory cells located within tumor and other normal tissues. Thus, while there was no obvious infectious process in these patients, we are not certain of the cellular location of the FDG uptake in the lung.

While FDG uptake in normal lung is quite low relative to many untreated tumors, there is clearly regional variability in supine humans. To the best of our knowledge, there exists no prior report on differential regional FDG uptake in normal lung. Similar to reports regarding other aspects of lung physiology, we found a significant ventrodorsal and craniocaudal difference in regional FDG uptake in the normal lungs in the reported 31 cases studied in the supine position. Since we retrospectively analyzed regional SUVs in normal lung, data for the prone position were not obtained. SUVs may change with the time of measurement; however, the measurement interval from 50 to 70 min was short, and the locations at which SUVs were measured were mixed. Thus, the significant differences in mean SUVs were not caused by differences in time of measurement. FDG is transported from the blood to the tissues by a carrier-mediated diffusion mechanism. Hexokinase catalyzes the phosphorylation of FDG to FDG-6-PO_4, and FDG-6-PO_4 is metabolically trapped in the tissues. Blood FDG activity is generally low. The tissue uptake of the FDG is dependent upon blood flow, glucose metabolism and tissue density. Therefore, the ventrodorsal gradient in regional pulmonary FDG uptake is probably multifactorial but possibly delivery related. We also should not forget the predominant FDG uptake in the myocardium and the liver. Scatter from these organs might contribute to the increased FDG uptake in the lower lungs. However, there was no significant difference in mean SUVs be-

tween the right and left lobes in the lower lung field; furthermore, the contribution of scatter to total image counts is viewed as relatively modest in 2D PET. We ourselves did not see obviously high ^{18}F activity in lung adjoining the heart (which generally had low activity) in these fasted patients, though the SUV in the mid portion of the left middle lung was slightly greater than that on the right.

As regards lesion detectability, more study is needed to determine whether lower lung lesions are more difficult to detect than those more cranially located, in the upper lung. Loss of count recovery can occur due to insufficient z-axis sampling and x-y- and z-axis reconstructed resolution elements greater than tumor size [23]. Our previously reported failure to detect several small lower lobe metastases of melanoma with an older ECAT 931 scanner may partly be due to its poorer z-axis resolution and sampling as compared with various newer scanners. The mean SUV for primary lung cancer lesions is 9.44 in our institution [24]. Assuming a spherical lesion of 5 mm in diameter with a true SUV of 9.44 and a reconstructed system resolution of 1 cm, the recovery coefficient for such a lesion would be about 0.05 [23]. So the measured SUV for this lesion would be 0.472, which is lower than normal lung SUVs obtained from this study. This calculation supports our observation that it is difficult to detect small lesions with many PET scanners, especially when such lesions are located in the lower and/or posterior lung fields with increased background activity. An additional contributing factor could be motion of the lungs during respiration. It is quite probable, however, that the somewhat higher background activity in the posterior and/or lower lung fields could make the detection of small lesions more difficult in these locations.

In conclusion, background ^{18}F activity is significantly increased in the posterior and lower lungs as compared with the upper and anterior lungs. This increased background, along with other factors, may contribute to occasional false-negative findings in these areas, particularly for small lesions. Increased blood flow and FDG delivery, increased blood volume, and also scatter from heart and liver may contribute to the increased lung background activity. Regional differences in normal lung FDG uptake, while modest, are significant and should be considered when interpreting PET studies in patients with suspected primary or metastatic lung cancer. The regional variation in ^{18}F uptake may be of greatest impact in assessing small lower lobe pulmonary lesions, especially if a high-resolution PET scanner is not used.

Acknowledgements. This work was financially supported by NCI grant CA56731-02 and Mitsubishi Research Institute Inc.

References

1. Warburg O, Posener K, Negelein E. The metabolism of the carcinoma cell. In: *The metabolism of tumors.* New York: Richard R. Smith; 1931: 29–169.
2. Weber G. Enzymology of cancer cells (first of two parts). *N Engl J Med* 1977; 296: 486–492.
3. Weber G. Enzymology of cancer cells (second of two parts). *N Engl J Med* 1977; 296: 541–551.
4. Wahl RL, Hutchins GD, Buchsbaum DJ, Liebert M, Grossman HB, Fisher S. 18F-2-deoxy-2-fluoro-D-glucose uptake into human tumor xenografts. Feasibility studies for cancer imaging with positron-emission tomography. *Cancer* 1991; 67: 1544–1550.
5. Gritters LS, Francis IR, Zasadny KR, Wahl RL. Initial assessment of positron emission tomography using 2-fluorine-18-fluoro-2-deoxy-D-glucose in the imaging of malignant melanoma. *J Nucl Med* 1993; 344: 1420–1427.
6. Toorongian SA, Mulholand GK, Jewett DM, Bachelor MA, Kilbourn MR. Routine production of 2-deoxy-2[F-18]fluoro-D-glucose by nucleophilic exchange on a quaternary 4-aminopyridinium resin. *Int J Rad Appl Instrum [B]* 1990; 17: 273–279.
7. Wahl RL, Cody RL, Hutchins GD, Mudgett EE. Primary and metastatic breast carcinoma: initial clinical evaluation with PET with the radiolabeled glucose analogue 2-[F-18]-fluoro-2-deoxy-D-glucose. *Radiology* 1991; 179: 765–770.
8. Wahl RL, Harney J, Hutchins G, Grossman HB. Imaging of renal cancer using positron emission tomography with 2-deoxy-2-(^{18}F)-fluoro-D-glucose: pilot animal and human studies. *J Urol* 1991; 146: 1470–1474
9. Newman JS, Francis IR, Kaminski MS, Wahl RL. Imaging of lymphoma with PET with 2-[F-18]-fluoro-2-deoxy-D-glucose: correlation with CT. *Radiology* 1994; 190: 111–116.
10. Zasadny KR, Wahl RL. Standardized uptake values of normal tissues at PET with 2-[fluorine-18]-fluoro-2-deoxy-D-glucose: variations with body weight and a method for correction. *Radiology* 1993; 189: 847–850.
11. Yonekura Y, Benua RS, Brill AB, Som P, Yeh SD, Kemeny NE, Fowler JS, MacGregor RR, Stamm R, Christman DR, Wolf AP. Increased accumulation of 2-deoxy-2-[^{18}F]fluoro-D-glucose in liver metastases from colon carcinoma. *J Nucl Med* 1982; 23: 1133–1137.
12. Nolop KB, Rhodes CG, Brudin LH, Beaney RP, Krausz T, Jones T, Hughes JM. Glucose utilization in vivo by human pulmonary neoplasms. *Cancer* 1987; 60: 2682–2689.
13. Ichiya Y, Kuwabara Y, Otsuka M, Tahara T, Yoshikai T, Fukumura T, Jingu K, Masuda K. Assessment of response to cancer therapy using fluorine-18-fluorodeoxyglucose and positron emission tomography. *J Nucl Med* 1991; 32: 1655–1660.
14. Okada J, Yoshikawa K, Imazeki K, Minoshima S, Uno K, Itami J, Kuyama J, Maruno H, Arimizu N. The use of FDG-PET in the detection and management of malignant lymphoma: correlation of uptake with prognosis. *J Nucl Med* 1991; 32: 686–691.
15. Wahl RL, Quint LE, Cieslak RD, Aisen AM, Koeppe RA, Meyer CR. "Anatometabolic" tumor imaging: fusion of FDG PET with CT or MRI to localize foci of increased activity. *J Nucl Med* 1993; 34: 1190–1197.
16. Wahl RL, Quint LE, Greenough RL, Meyer CR, White RI, Orringer MB. Staging of mediastinal non-small cell lung cancer with FDG PET, CT, and fusion images: preliminary prospective evaluation. *Radiology* 1994; 191: 371–377.
17. Millar AB, Denison DM. Vertical gradients of lung density in healthy supine men. *Thorax* 1989; 44: 485–490.
18. Verschakelen JA, Van Fraeyenhoven L, Laureys G, Demedts M, Baert AL. Differences in CT density between dependent and nondependent portions of the lung: influence of lung volume. *Am J Roentgenol* 1993; 161: 713–717.

19. Rosenblum LJ, Mauceri RA, Wellenstein DE, Thomas FD, Bassano DA, Raasch BN, Chamberlain CC, Heitzman ER. Density patterns in the normal lung as determined by computed tomography. *Radiology* 1980; 137: 409–416.
20. Wollmer P, Albrechtsson U, Brauer K, Eriksson L, Jonson B, Tylen U. Measurement of pulmonary density by means of X-ray computerized tomography. Relation to pulmonary mechanics in normal subjects. *Chest* 1986; 90: 387–391.
21. Schuster DP, Marklin GF, Mintun MA, Ter-Pogossian MM. PET measurement of regional lung density: 1. *J Comput Assist Tomogr* 1986; 10: 723–729.
22. Rhodes CG, Wollmer P, Fazio F, Jones T. Quantitative measurement of regional extravascular lung density using positron emission and transmission tomography. *J Comput Assist Tomogr* 1981; 5: 783–791.
23. Kessler RM, Ellis J Jr, Eden M. Analysis of emission tomographic scan data: limitations imposed by resolution and background. *J Comput Assist Tomogr* 1984; 8: 514–522.
24. Wahl RL, Zasadney KR, Strand BL, Minn HRI. FDG-PET in patients with untreated breast cancers and untreated lung cancers: comparison of FDG uptake and influx [abstract]. *J Nucl Med* 1995; 36: 83P.